

Using Numerical Simulation and Nanoindentation for Determining the Plastic-Viscoplastic Mechanical Properties of Thin Films

利用奈米壓痕儀和有限元素法萃取薄膜的塑 —黏塑性之機械性質

陳峯元

Feng-Yuan Chen

黎明技術學院創意產品設計系

Department of Innovative Product Design, Lee-Ming Institute of Technology

張瑞慶

Rwei-Ching Chang

聖約翰科技大學機械與電腦輔助系

Department of Mechanical and Computer-Aided Engineering, St. John's University

Abstract

In this paper, a three side pyramidal Berkovich probe tip was used in nanoindentation test and finite element method (FEM) was taken to simulate and determine the mechanical properties of the Ti film on Si substrate. The elastic-perfectly plastic and viscoplastic material properties were employed in the FEM to reproduce the load-depth curves of nanoindentation. The results showed that comparison of the experimental data and numerical results demonstrated that finite element approach is capable of reproducing the load-depth curves of nanoindentation test and while the viscoplastic material properties are adopted in the FEM analysis, the load-depth curves of numerical simulation are very close to the experimental curves.

Key Words: Nanoindentation, FEM, elastic-plastic, viscoplastic, thin films.

摘 要

本文利用金字塔狀之貝克維奇奈米探針的奈米壓痕儀實驗和有限元素法數值模擬來模擬並萃取矽基鍍鈦薄膜之機械性質。文中利用有限元素法並假設鈦薄膜之機械性質分別為彈完全塑性或黏塑性，重建由奈米壓痕儀實驗所取得



之作用力與變形量曲線。研究結果顯示，比較實驗與有限元素法的結果，發現有限元素法可以模擬出奈米壓痕儀實驗所取得之作用力與變形量曲線。尤其當鈦薄膜之機械性質假設為黏塑性材料時，有限元素法模擬出的作用力與變形量曲線與奈米壓痕儀實驗所取得的曲線非常吻合。

關鍵詞：奈米壓痕儀實驗、有限元素法、彈完全塑性、黏塑性、薄膜



1. INTRODUCTION

Numerical simulations play an important role in recent technology developments. The FEM has been proved as a powerful tool in the nanoindentation simulation. Lichinchi [1] have simulated nanoindentation of TiN film on HSS by using FEM, and both axisymmetric and three-dimensional models were employed. They concluded that both models are similar and provide good fit. Ma [2] employed the FEM to simulate the indentation test for Al film on Si substrate, and to determine the mechanical properties of the films by combining calculation with nanoindentation test. Pelletier [3] have investigated the influence of material bilinear elastic-plastic behaviour model for numerical simulation of nanoindentation testing of various bulk metals. They concluded that different pairs of yield strength and plastic modulus can produce a good fit to the experimental results of load versus displacement.

In this paper, the FEM was used to simulate the nanoindentation test for Ti films on Si substrate. The elastic-perfectly plastic and viscoplastic material properties were employed in the FEM to reproduce the nanoindentation load-depth curves. The results compared with both calculation solution and experimental data.

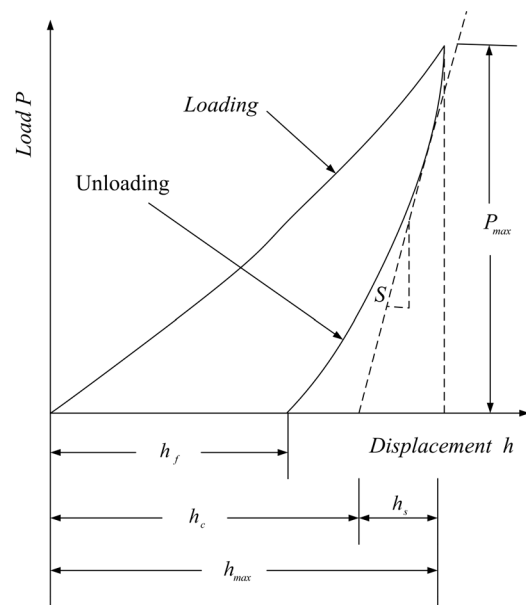


Fig. 1 schematic representation for load-depth data for a nanoindentation experiment

2. Nanoindentation

The Ti film on Si substrate were studied with a high-resolution nanomechanical test instrument which is a nanoindenter (Triboscope, Hysitron) assembled on an atomic force microscope (Autoprobe, CP-Research), and a three side pyramidal Berkovich probe tip is used in the test. Five indentations were made in each sample at the same maximum loads. Nanoindentation is performed under a precisely continuous measurement of the load and the depth during the test. Fig. 1 shows a schematic draw of an indentation load via depth curve.

In the Oliver and Pharr [4] method, the hardness H and the reduced modulus E_r are derived from

$$H = \frac{P_{\max}}{A} \quad (1)$$

and

$$\left(\frac{dP}{dh}\right)_{\text{unload}} = S = 2\beta E_r \sqrt{\frac{A}{\pi}} \quad (2)$$

where P_{\max} is the maximum indentation load, A is the projected contact area, S is the unloading stiffness measured at maximum depth of penetration h , β is a constant that depends on the geometry of the indenter, for Berkovich indenter $\beta = 1.034$. The reduced modulus is used in the analysis to take into account that elastic deformation occurs in both the indenter and the specimen and it is given by

$$\frac{1}{E_r} = \frac{1-\nu^2}{E} + \frac{1-\nu_i^2}{E_i} \quad (3)$$

where E , E_i and ν , ν_i are the elastic modulus and Poisson's ratio of the indenter and the specimen material, respectively. For evaluating the elastic modulus E_r , the slope $\left(\frac{dP}{dh}\right)_{\text{unload}}$ and the contact area A should be determined precisely. A least mean square fit to 90% of the unloading curve is made according to the hypothesis that the unloading data will be expressed by a power law

$$P = P_{\max} \left(\frac{h - h_f}{h_{\max} - h_f}\right)^m \quad (4)$$

For an indenter with a known geometry, the projected contact area is a function of the contact depth. The area function for a perfect Berkovich indenter is given by

$$A = f(h_c) = 24.56h_c^2 \quad (5)$$

Indenters used in practical nanoindentation testing are not ideally sharp. Therefore, tip geometry calibration or area function calibration is needed. A series of indentations is made on fused quartz at depths of interest. A plot of A versus h_c can be curve fit according to the following functional form

$$A = f(h_c) = 24.56h_c^2 + C_1h_c^1 + C_2h_c^{1/2} + C_3h_c^{1/4} + \dots + C_8h_c^{1/128} \quad (6)$$

where C_1 through C_8 are constants. The lead term describes a perfect Berkovich indenter.

3. Numerical Simulation

In this study, a commercial finite element code ANSYS was used to reproduce the load-depth curves of the Ti film on Si substrate in the nanoindentation process and both the elastic-perfectly plastic and viscoplastic materials are considered individual. An axisymmetric cone with half-included angle of 70.3° which the conical indenter has the same area function as a Berkovich tip [3] was used in this study and the Plan42, Conta171 and Targe169 elements were adopted. Fig. 2 and 3 show the axisymmetric mesh and boundary conditions. As the reported by Lichinchi [1], three-dimensional model was compared with two-dimensional axisymmetric model, no relevant differences are apparent between the two models. Therefore, we have chosen the two-dimensional axisymmetric model in order to restrain the degrees of freedom.



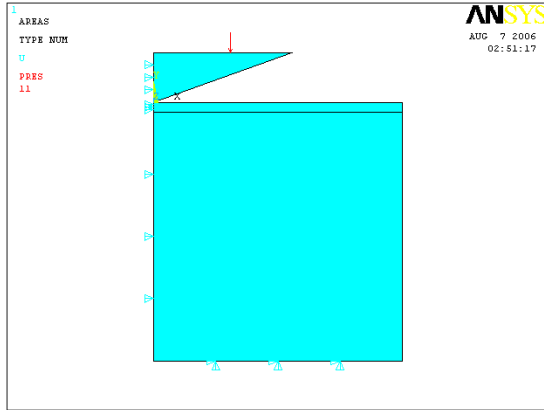


Fig. 2 an axisymmetric cone with half-included angle of 70.3° in which the conical indenter has the same area function as a Berkovich tip

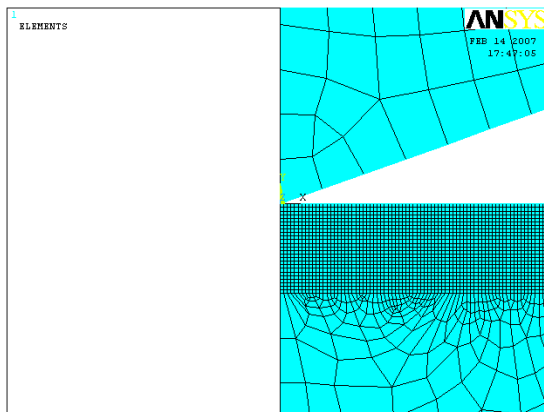


Fig. 3 the axisymmetric mesh

In our work, the Berkovich diamond tip was used and simulated as a perfectly elastic material with elastic modulus of 1140 GPa and Poisson's ratio of 0.07. The silicon substrate was modeled as a perfectly elastic material with elastic modulus of 127 GPa and Poisson's ratio of 0.278 [2]. The Ti film was modeled as the elastic-perfectly plastic (Fig. 5) or viscoplastic materials individual and both elastic modulus were obtained by nanoindentation and equation (1)-(6). While

the elastic-perfectly plastic material was employed at FEM, the yield stress S_y must be changed for reproducing the experimental load-depth curve, and while viscoplastic material was considered at FEM, the Perzyna model is used and given by

$$\sigma = \left[1 + \left(\frac{\dot{\epsilon}^{pl}}{\gamma} \right)^m \right] S_y \quad (7)$$

where σ is material yield stress, $\dot{\epsilon}^{pl}$ is equivalent plastic strain rate, γ is material viscosity parameter, m is strain rate hardening parameter and S_y is static yield stress of material. As γ tends to ∞ , or m tends to zero or $\dot{\epsilon}^{pl}$ tends to zero, the solution converges to the static (rate-independent) solution. However, for this material option when m is very small (< 0.1), the solution shows difficulties in convergence. Finally, the strain rate hardening parameter m and the material viscosity parameter γ are able to change at FEM for reproducing the experimental load-depth curve.

4. Result and discussion

Using the Oliver and Pharr [4] method, the elasticity modulus and hardness can be determined by their method in nanoindentation, but yield stress and other material properties, such as work-hardening rate, cannot be obtained. For determining the yield stress and other material properties, the FEM was used to simulate the nanoindentation test to produce the experimental load-depth curves.



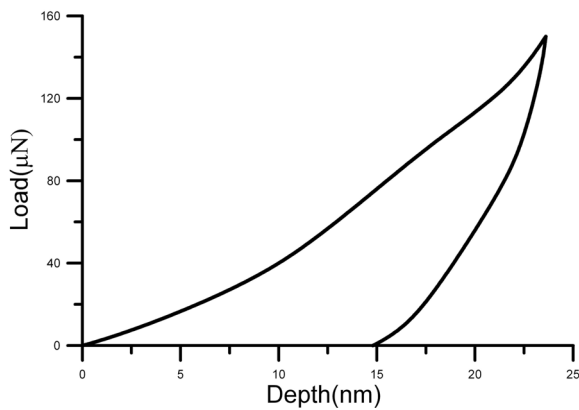


Fig. 4 the load-depth curve due to nanoindentation test

At first, there are five indentations to conduct at each penetration depth in the nanoindentation, and the experimental results represent average values or load-depth curves for all materials. The maximum load was 150 μN and the thickness of Ti film was deposited 200 nm, and the thickness of Si substrate was about 35 μm . The penetration depth is chosen not to exceed 20 % of the film thickness in order to avoid substrate effects [1]. In Fig. 4, it shows that the load-depth curve due to nanoindentation test. The elastic modulus E of the thin film can be calculated from eq. (1)-(6) and obtained $E=150$ GPa, and the value of the Poisson' ratio found in literature $\nu=0.25$ [2].

Second, the material properties were assumed to be elastic-perfectly plastic (Fig. 5), where S_y is the static yield stress. Fig. 6 presents the load-depth curves in different yield stress S_y (6, 7.5 and 9 GPa), where the linear elastic modulus is $E=150$ GPa and force is $P=150$ μN . The load-depth curve

includes loading and unloading parts. The Fig. 7 shows that the unloading curve of simulation by FEM shifts to the right as $S_y < 7.5$ Gpa and shifts to left as $S_y > 7.5$ Gpa with the experimental curve and while $S_y=7.5$ GPa the unloading curve of simulation by FEM is very close to the experimental curve. But all of the loading curves of simulation by FEM shifts to the right and exists the large deviation with the experimental curve.

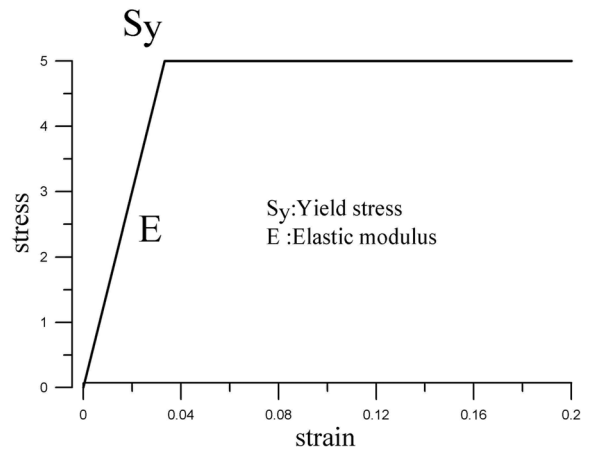


Fig. 5 the stress-strain curve of the elastic-perfectly plastic material

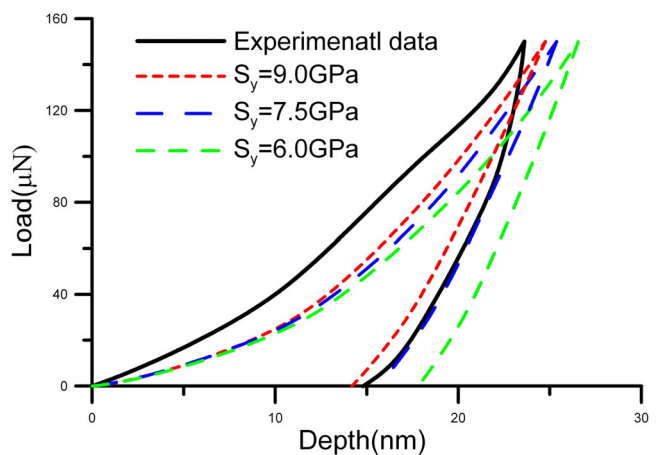


Fig. 6 the load-depth curves by nanoindentation and FEM in different yield stress S_y



Finally, the material properties were assumed to be viscoplastic material in FEM and the Perzyna model (equation 7) is used. The static yield stress S_y , material viscosity parameter γ and strain rate hardening parameter m are unknown, and they are allowed to change within a reasonable range prior to determining them. Fig. 7 is the load-depth curves by nanoindentation and FEM in different strain rate hardening parameter m , at material viscosity parameter $\gamma = 1.0$, static yield stress $S_y = 7.5 \text{GPa}$. It shows that comparison with the experimental curve, the unloading curves shift left as the strain rate hardening parameter $m > 0$, and when $m = 1.0$ the curve shift more left than the curve as $m = 0.5$. It is the rate-independent plastic as $m = 0$. For loading curves both $m = 0.5$ or 1.0 , the curves shift left from the curve of $m = 0$ and more close to experimental data. Fig. 8 shows the same phenomenon as $S_y = 6.0 \text{GPa}$.

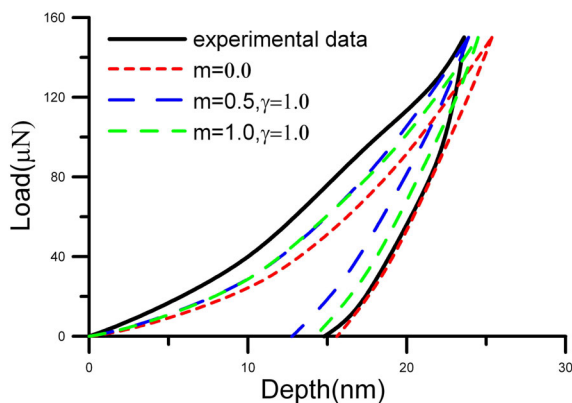


Fig. 7 the load-depth curves by nanoindentation and FEM in different strain rate hardening parameter m and yield stress $S_y = 7.5 \text{GPa}$

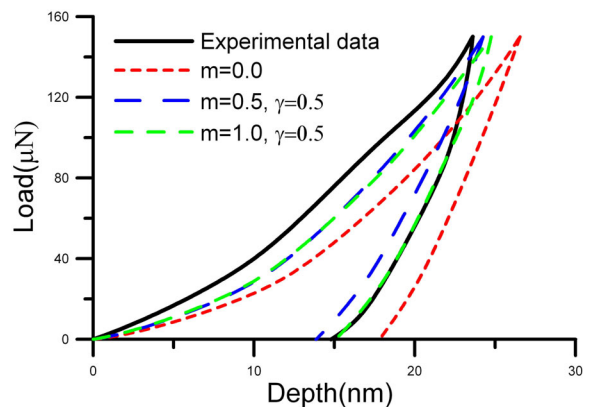


Fig. 8 the load-depth curves by nanoindentation and FEM in different strain rate hardening parameter m and yield stress $S_y = 6.0 \text{GPa}$

Fig. 9 shows the load-depth curves by nanoindentation and FEM in different material viscosity parameter γ , at strain rate hardening parameter $m = 1.0$ and static yield stress $S_y = 6.0 \text{GPa}$. Both loading and unloading curves are shift left as $\gamma < 1.0$, and the smaller viscosity parameter γ , the more the curve shifts.

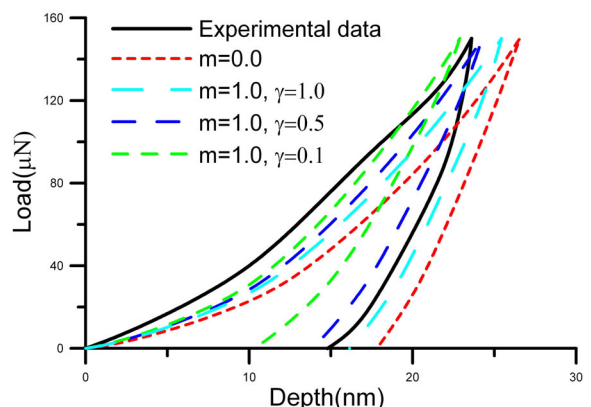


Fig. 9 the load-depth curves by nanoindentation and FEM in different material viscosity parameter γ , and static yield stress $S_y = 6.0 \text{GPa}$



According to the above discussion, using the FEM to reproduce the load-depth curves of nanoindentation was employed by different material properties. While the elastic-perfectly plastic material was used at numerical simulation and the yield stress S_y is 7.5Gpa, the load-depth curves of numerical simulation agree well with the experimental data. And while the material properties are assumed to be viscoplastic material in FEM and the Perzyna model is used. The load-depth curves of numerical simulation agree well with the experimental data when the strain rate hardening parameter $m=1.0$, material viscosity parameter $\gamma=0.5$ and static yield stress $S_y=6.0$ Gpa are adopted in the FEM analysis.

5. Conclusions

FEM simulation with the commercial software ANSYS was used to reproduce the load-depth curves of the Ti film on Si substrate in the nanoindentation and both the elastic-perfectly plastic and viscoplastic materials are considered individual. The numerical results are compared with the experimental data, and the following conclusions are obtained.

- (1) Comparison between the experimental data and numerical results demonstrated that finite element approach is capable of reproducing the loading-unloading behavior of a nanoindentation test.
- (2) While the elastic-perfectly plastic material was used at numerical

simulation and the yield stress S_y is 7.5Gpa, the load-depth curves of numerical simulation agree well with the experimental data.

- (3) While the material properties are assumed to be viscoplastic material in FEM and the Perzyna model is used. The load-depth curves of numerical simulation agree well with the experimental data when the strain rate hardening parameter $m=1.0$, material viscosity parameter $\gamma=0.5$ and static yield stress $S_y=6.0$ Gpa are adopted in the FEM analysis.

REFERENCES

1. M. Lichinchi, C. Lenardi, J. Haupt and R. Vitali, "Simulation of Berkovich nanoindentation experiments on thin films using finite element method", *Thin Solid Films* 312, 1998, pp.240-248.
2. D. Ma, K. Xu and J. He, "Numerical simulation for determining the mechanical properties of thin metal films using depth-sensing indentation technique", *Thin Solid Films* 323, 1998, pp.183-187.
3. H. Pelletier, J. Krier, A. Cornet and P. Mille, "Limits of using bilinear stress-strain curve for finite element modeling of nanoindentation response on bulk materials", *Thin Solid Films* 379, 2000, pp.147-155.
4. W.C. Oliver and G.M. Pharr "An improved technique for determining hardness and elastic-modulus using load and displacement sensing indentation experiments", *J. Mater. Res.*, 7, 1992, pp. 1564-83.

